JEAS

JOURNAL OF ENGINEERING AND APPLIED SCIENCES

Journal of Engineering and Applied Sciences, Volume 20, Number 1, June 2022, 738 - 752

Mitigation of Corrosion of Al-Si-Ti based Alloy in 1 M KOH Solution using Imidazolium-Based 1- BUTYL-3-Methylimidazolium Chloride

Udunwa D. I[1*], and Onukwuli O. D[2]. Njoku, C. N[3]

[1*]Department of Polymer and Textile Engineering, Federal University of Technology, Owerri Imo State, Nigeria
[2]Department of Chemical Engineering, Nnamdi Azikiwe University, Awka, Anambra State, Nigeria
[3]Department of Chemical Engineering, Federal University of Technology, Owerri, Imo state, Nigeria
*Corresponding Author's E-mail addresses: udunwadaniel@gmail.com

Abstract

The corrosion inhibition characteristics of 1-butyl-3-methylimidazolium chloride ([BMIM][Cl]) ionic liquid (IL) on Al-Si-Ti based alloy (AA) immersed in 1 M KOH solution were investigated at different solution temperatures of 303 - 343 K, inhibitor concentrations of 0.2 - 1.0 g/L and maximum immersion time of 3 hrs. using electrochemical (EIS), potentiodynamic polarization (PDP) and thermometric methods, respectively. The inhibition efficiency (IE %) was evaluated by estimating the corrosion current densities (i_{corr} ($\mu A/cm^2$)) and the charge transfer resistance ($R_{(t)}$ ($\Omega\ cm^2$)) in the absence and the presence of [BMIM][Cl] for the potentiodynamic polarization (PDP) and electrochemical impedance spectroscopy (EIS) techniques. Reaction number (RN) in the blank and the inhibited solution was compared and employed for the calculation of the inhibition efficiency for the thermometric studies. Maximum inhibition efficiencies of 86.76 %, 82.10 % and 70.80 % were obtained from thermometric, Potentiodynamic polarization and electrochemical impedance spectroscopy at concentration of 1.0 g/L [BMIM][Cl] and temperature of 303 K, respectively. In all, the inhibition efficiency of the IL inhibitor increases with an increase in the dosage of [BMIM][Cl] administered and decreases with rise in temperature. The adsorption process of the inhibitor molecules on the surface of AA obeyed the Langmuir adsorption isotherm at all concentration of [BMIM][Cl] and temperature investigated. A physisorption operation was proposed for the inhibition behaviour of the ionic liquid inhibitor from the calculated values of the heat of adsorption and free energy of adsorption.

Keywords: [BMIM][Cl], KOH, aluminium alloy, physisorption operation, inhibited solution.

1.0 Introduction

Aluminium and its alloys are considerably used in the manufacturing, construction and engineering industries. It is one of the lightest metal commercially available and has an inherent high strength to weight ratio (Singh and Quraishi, 2012). The addition of alloying elements like magnesium, copper, silicon and manganese help to increase the tensile strength of aluminium and produce an alloy with desirable properties which is designed for particular applications (Deepa and Padmalatha, 2014). Apart from the addition of alloying elements to the metal to improve its property, the oxide of aluminium is one of the most stable of all oxides and it is difficult to reduce (Nnanna et al, 2011; Chigoziri et al, 2015). This is why aluminium sheets are mainly used as roofing materials in buildings or used as protective covering on material in engineering application where part or whole of the body of the material is exposed to the environment. In strong alkaline solution a gradual introduction of the hydroxyl groups to surface of aluminium atoms, with the eventual formation of $Al(OH)_4$ results to loss of metal to corrosion and degradation (Namrata et al, 2017; Okafor et al, 2019).

The consistent dependency on aluminium can be easily disrupted during performance by either internal or external factors through a phenomenon known as corrosion. Corrosion causes huge economic losses by aiding the failure of many structural and engineering works. Therefore, corrosion can be defined as ‘’irreversible and spontaneous deterioration of metal or alloy through chemical or electrochemical reaction with the environment’’ (Onukwuli and Ezeugo, 2018; Asadi et al, 2019). Due to the ugly effects of corrosion highlighted, corrosion is an unpleasant phenomenon that have to be prevented or reduced. Scientists and researchers has suggested and executed different methods of controlling and protecting metal surfaces from corrosion (Ndibe et al, 2011).

Amidst these methods, the use of corrosion inhibitors which is regarded as one of the best corrosion inhibition method (Ejikeme et al, 2015). A corrosion inhibitor is a chemical, organic or mixture of substances that when added to an aggressive environment in a small quantity successively retard or inhibit corrosion process without linking with the environmental component (Devarayan et al, 2012; Omotioma and Onukwuli, 2016). Therefore, inhibitors are used in industrial and commercial processes to reduce metal degradation. Organic and inorganic compounds constitute a large class of corrosion inhibitors, which affects the entire surface of the corroding metal when present in sufficient concentration (Onukwuli and Omotioma, 2019). Most of the organic or synthetic compounds containing functional groups of the type amine, carbonyl and alcoholic groups are more effective corrosion inhibitors (Verma et al, 2019). Amitha and Bharathi, (2011) noted that most organic compound containing heterocyclic base compounds containing oxygen, sulphur, nitrogen with multiple bonds have been reported as good corrosion inhibitors and exhibit significant inhibition efficiency. Despite the good results obtained before, most of these compounds (chemical and synthetic inhibitors) produces immunological response when exposed to the body or body fluids and are not economically cost effective. The growing knowledge of health, safety and environment has pinched researcher’s awareness to develop very dominant and productive environmentally friendly inhibitors as the ionic liquids (ILs) (Verma et al, 2018; Dehghani et al, 2019). Ionic liquids can be regarded as greener chemicals due to their negligible vapour pressure, pH stability, non-flammability and high chemical and thermal stability (Sasikumar et al, 2015; Verma et al, 2019). These attribute of the compound has promoted the investigation of more ionic liquids as potential of corrosion inhibitors (Verma et al, 2019). The limitation of the use of conventional organic and polymeric compounds as corrosion inhibitors due to low solubility in polar electrolytic media is readily overcome by the use of ionic liquids (Verma et al, 2017; Chauham et al, 2021). The ionic liquids contain unsaturated functional groups such as C = C, C = O, -N=N, -C=S, -N=O, -C-C- and –C-N, π-electrons as well as non-bonding electrons of heteroatoms (N, O, S and P) and hence, facilitate the adsorption of their molecules on the surface of the metals (Li et al, 2019; Verma et al, 2019).

There are rigorous studies on the use of ionic liquids as corrosion additives under aggressive environments.
The inhibition behaviour of 1,3-bis (2-oxo-2-phenylethyl)-1H-imidazol-3-ium bromide (OPEIB) on 6061 Al-15 vol. pct. SiC (p) composite in 0.1 M H_2SO_4 solution was studied by Shetty and Shetty (2015) using EIS and PDP methods. The investigated ionic liquid exhibits the maximum efficiencies of 96.7 and 94 % using PDP and EIS methods, respectively. Potentiodynamic polarization study further reveals that studied IL behaves as cathodic type inhibitor and its adsorption on the composite surface followed the Temkin adsorption. Zhang and Hua, (2010) studied the effect of 1-hexyl-3-methylimidazolium (HMIC) and 1-octyl-3-methylimidazolium chlorides (OMIC) on aluminium corrosion in 1 M HCl using electrochemical and weight loss methods results showed that inhibition efficiencies of these ILs increase with increasing their concentration and obeyed the order: OMIC > HMIC. Potentiodynamic study revealed that the ionic liquids acted as mixed type inhibitors and their adsorption on aluminium surface followed the Langmuir adsorption isotherm. Also, Li et al, (2011) studied the inhibition behaviour of tetradecylpyridinium bromide (TDPB) on aluminium corrosion in 1 M HCl solution using weight loss and electrochemical methods. Results of the investigation showed that TDPB inhibits the aluminium corrosion by adsorbing on the metallic surface. The adsorption of the TDPB followed the Langmuir adsorption isotherm. Polarization study suggested that TDPB acts as cathodic type inhibitor for acidic aluminium corrosion.

The above literature analysis high points the significance of identifying effective corrosion inhibitors for aluminium and its alloy in order to increase safety, minimize maintenance costs and limits the use of toxic inhibitors when it is embraced, mostly in the industries, chemical plants, or for flow systems experiencing acute alkaline attack (Namrata et al, 2017). The imidazolium-based ionic liquids have been accepted as one of the biocompatible, inexhaustible and non - toxic corrosion inhibitors that will replace the harmful synthetic and chemical corrosion inhibitors. This present study is designed to study the corrosion inhibitory performance of novel 1-butyl-3-methylimidazolium chloride [BMIM][Cl] for Al-Si-Ti based alloy (AA) in 1 M KOH solution using thermometric, potentiodynamic polarization and electrochemical impedance spectroscopy techniques.

1-butyl-3-methylimidazolium chloride ([BMIM][Cl]) is an imidazole - based ionic liquid with a high molecular weight and is used as a green and neutral reaction media for the efficient catalyst free synthesis of quinoxaline derivatives. Quinoxaline possess various biological activities, such as antimycobacterial, antibacterial, antifungal, antitumor, antidepressant and also used in dye production. In medicine [BMIM][Cl] has shown the ability to inhibit the growth of pathogenic and nonpathogenic bacteria and fungi. Dye is used to add colour and printing on fabrics, fibers, garments by strongly bonding on the surface of materials to resist washing and friction. The high molecular weight of [BMIM][Cl], quick response to bacterial and fungal attack and its excellent bonding on materials (as dye component) could be seen as an advantage in corrosion inhibition and adequate surface coverage of metals. Fig. 1 exhibits the molecular structure of [BMIM][Cl]. The ionic liquid (IL) is adsorbed on the surface of the metal there by blocking the active reaction sites on the metal surface by forming a thick layer on the surface of the metal and hence retards the corrosion of the metal alloy (Verma et al, 2019).

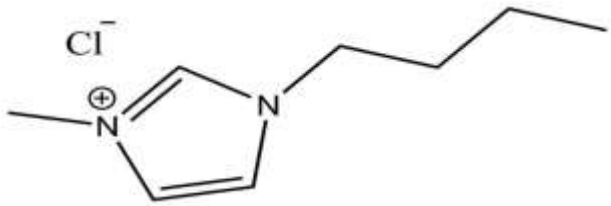

Fig. 1: Structure of 1-butyl-3-methylimidazolium chloride

2.0 Material and methods

2.1 Preparation aluminium alloy

Aluminium alloy (AA) sheet of composition; Si (0.25 %), Fe (0.02 %), Zn (0.07 %), Mn (0.14 %) Mg (0.03 %), V (0.04 %), Ti (0.12 %), Cu (0.03 %), Al (99.3 %) was obtained from Innoson Aluminium Nig. Ltd Aba, Abia State. The AA sheet (75 cm x 75 cm x 0.06 cm) was mechanically pressed cut into different coupons size of dimensions 3cm x 3cm x 0.06cm (with 96% reduction rate). Each coupon was abraded using 400, 800 and 1200 emery sand paper to obtain a smooth and uniform surface area, polished and drilled at one end and numbered by mechanical punching. The numbered coupons were degreased by washing with ethanol, rinsed with acetone and allowed to dry in air before it was preserved in the desiccator to avoid contact with moisture.

2.1.2 Preparation of 1 M KOH

1 M KOH was prepared by dissolving 56 g of KOH in 1 litre of distilled water. All other chemicals used for the study were analytical grades and were used without further purification.

2.1.3 Synthesis of inhibitor (Ionic liquid) and concentration preparation

Mixture of 0.3 g n-methylimidazole and 0.35 g butyl chloride was placed in a microwave and irradiated for 7 minutes in the presence of toluene at the temperature of 110 ^{o}C at 80 % microwave power level. The product was collected and washed with dry ethyl acetate and dried overnight in an oven at 70 ^{o}C. The yield was white ionic liquid, 1-butyl-3-methyimidazolium chloride [BMIM][Cl] was 93.3 % pure. The inhibitor was synthesized and 20 grams of the inhibitor was dissolved in 1 L of the alkaline solution. From the stock solution (20 g/L), inhibitor test solution was prepared at concentrations of 0.2, 0.4, 0.6, 0.8 and 1.0 g/L.

2.2 FTIR Analysis

Cleaned and polished aluminium alloy (AA) samples was immersed in a 250 ml beaker containing solution of 1 M KOH for 3 hrs. in the absence and presence of the ionic IL inhibitor. At the end of the corrosion study, the corrosion products in the beakers were collected and kept inside the sample bottles. Small quantity of the corrosion products samples was collected and used to perform Fourier transform infrared spectrophotometer analysis using the thermos-scientific spectrophotometer SHMADZU, Model: 1R Affinity 1: S/N A 2137470136 Si. The functional groups of the corrosion products were determined. FTIR analysis of the pure sample of the IL was performed using same equipment and the functional groups of the pure sample of the IL were determined.

2.3 Structural Analysis

Small quantity of the synthesized IL was collected from the sample bottle and used to perform the gas chromatography mass spectrometry analysis utilizing the GC-MS equipment (Thermo Scientific Co. Japan) Thermo GC-TRACE ultra-version: 5.0. Thermo MS DSQ II. The interpretation of mass spectrum of GC-MS was done by using database of National Institute of Standard and Technology (NIST). The identification of compounds was accomplished by comparison of retention time (RT) and fragmentation pattern, as well as with mass spectra of the known component stored in the NIST library.

2.4 SEM Analysis

The surface morphology of the AA specimen was studied after immersion in the blank and inhibited solutions of 1 M KOH solution for 3 hr. at 1.0 g/L inhibitor concentration and temperature of 303 K. The scanning electron microscopy (Model-JEOL-JSM-6390) was used to obtain the images of AA coupons that was retrieved from the alkaline solution. The surface morphological characterization was carried out at the magnification 2.0 KX operated at an accelerating voltage 15 kV.

2.5 Corrosion Rate Measurement

2.5.1 Thermometric method

Thermometric measurements were carried out for AA using a thermostat set at 30 ^{o}C. The temperatures of the system containing the AA samples and the test solution (KOH) was recorded regularly until a steady temperature value was obtained. The reaction number for each set of experiment was determined using, Equation (1), (Omotioma and Onukwuli, 2016; Udeh et al, 2021).

$$RN = \left(T_m - T_i \middle/ t \right) {}^{o}C \middle/ \min \tag{1}$$

Where T_m and T_i are the maximum and initial temperatures in (^{o}C) respectively and t is the time in minutes elapsed to reach T_m.

The inhibitor efficiency was determined using, Equation (2) (Abiola et al, 2007).

$$IE\% = \left(1 - RN_i \middle/ RN_O \right) \times \frac{100}{1} \tag{2}$$

Where RN_O and RN_i are the reaction numbers for the metal dissolution in free and inhibited corrosive medium respectively.

2.5.2 Electrochemical measurement

The electrochemical measurement was carried out using a computer-controlled potentiostat (model Solar Tron ECI-1286) and the data was analyzed using frequency response analyzer (Solar Tron FRA-1286). A three electrode compartment having glass cell was used for the electrochemical measurements with a Platinum counter electrode and a saturated calomel electrode (SCE) as the reference electrode. A Teflon coated aluminium alloy cylinder, with surface prepared as described (Omotioma and Onukwuli, 2016; Talha et al, 2020) served as the working electrode. The measurement was carried out at 303 K and in the frequency range of 100 kHz to 0.01 Hz at the open circuit potential by super imposing a sinusoidal AC signal of small amplitude (10 mV). Potentiodynamic polarization (PDP) curves were obtained by changing the electrode potential automatically from -700 mV to -200 mV at a scan rate of 1.67 mVs^{-1}. The experiment was repeated for at least three times and the average best agreeing values reported for further statistical analyses. The inhibition efficiencies were calculated using the relationship Equation (3) and Equation (4), respectively (Deepa and Padmalatha, 2014; Namrata et al, 2017).

$$IE\% = \left(i_{ocorr} - i_{corr} \middle/ i_{ocorr} \right) \times \frac{100}{1} \tag{3}$$

$$IE\% = \left(R_{(t)} - R_{(to)} \middle/ R_{(to)} \right) \times \frac{100}{1} \tag{4}$$

Where $i_{0_{corr}}$ and i_{corr}, $R_{(to)}$ and $R_{(t)}$ are the corrosion current density in the absence of inhibitor, corrosion current density in the presence of the inhibitor, charge transfer resistance in the absence and charge transfer resistance in the presence of the inhibitor, respectively

3.0 Results and Discussions

3.1 FTIR Result of the Inhibitor and Corrosion Product

The FTIR analysis of synthesized [BMIM][Cl] is presented in Figure 1. The Figure revealed the presence of C-N stretch, C-C stretch, CH_3 stretch, C-H stretch, C=C stretch and halogen functional group. Figure 2 revealed the analysis of the corrosion inhibition products of AA in 1 M KOH with [BMIM][Cl]. Stretched C-C at 1155.5cm^{-1} peak, shifted to CH_3 at 1043.7cm^{-1} peak, C-H stretched at 1699.9cm^{-1} peak, shifted to C=O at 1636.3cm^{-1} peak and O-H stretched at 3391.9cm^{-1} peak shifted to O-H at 3368.8cm^{-1} peak with formation of IL/AA complex solution (Li et al, 2019; Dharaskar et al, 2013). The stretching and shifting of the peaks of the functional groups of the molecules of the inhibitor signifies the synergy among the functional groups in protecting the aluminium alloy from corroding in the alkaline medium (Eddy et al, 2011; Omotioma and Onukwuli, 2016). Disappearance of some of the functional group in the pure sample and the appearance of new functional groups depicts formation of a new compound during the electrochemical reaction proceed (Onukwuli and omotioma, 2016; Udunwa et al, 2017).

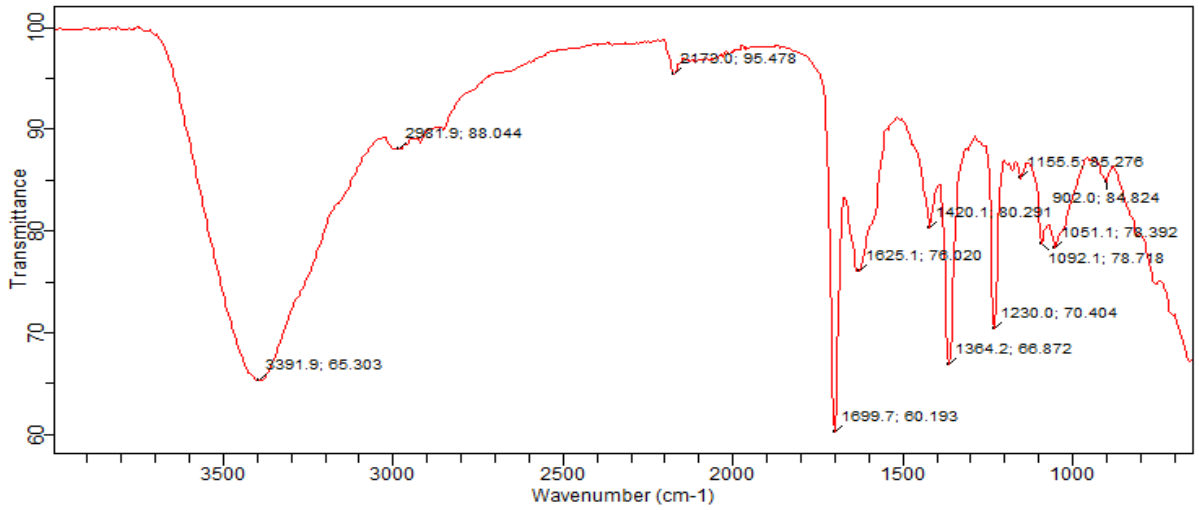

Fig. 1: FTIR spectra of [BMIM][Cl]

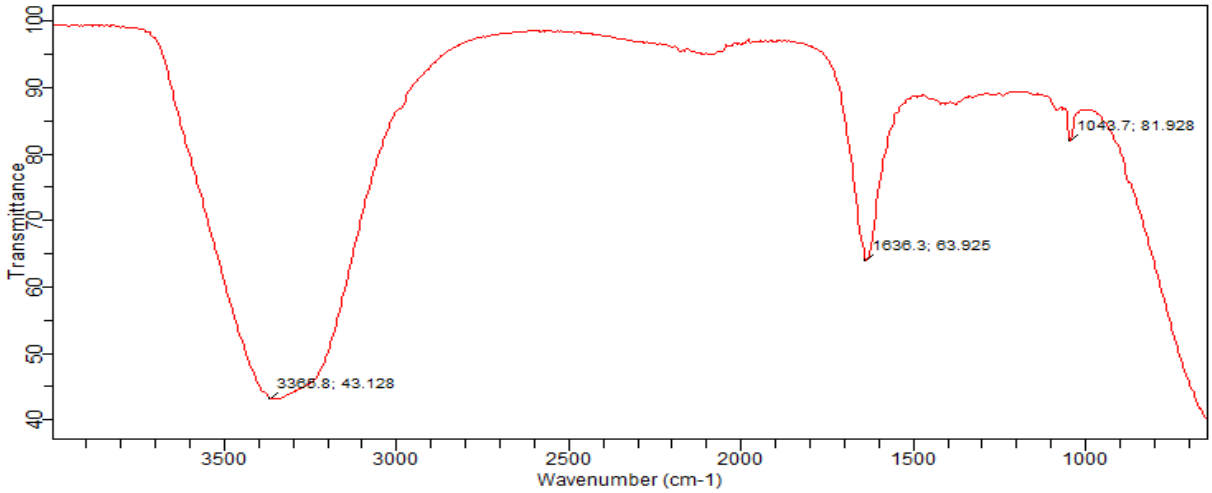

Fig. 2: FTIR spectra of AA in KOH with [BMIM][Cl]

3.2 GC-MS Analysis of [BMIM][Cl] Inhibitor

Interpretation of the mass spectrum of [BMIM][Cl] was done using database of National Institute Standard and Technology (NIST). The mass spectrum of the unknown component was compared with the spectrum of the known component stored in the NIST library. The relative percentage amount of each component was calculated by comparing its average peak area to the total areas. The major active constituents of [BMIM][Cl] are 4-piperidinone 2,2,6,6-tetramethyl, peak area (11.63%) and 2,4-Di-tert-butyl phenol peak area (49.91%) as shown by the chromatogram Figures 3 and 4. The chemical structures and physicochemical properties of these constituents make 1- butyl-3-methylimidazolium chloride a suitable corrosion inhibitor.

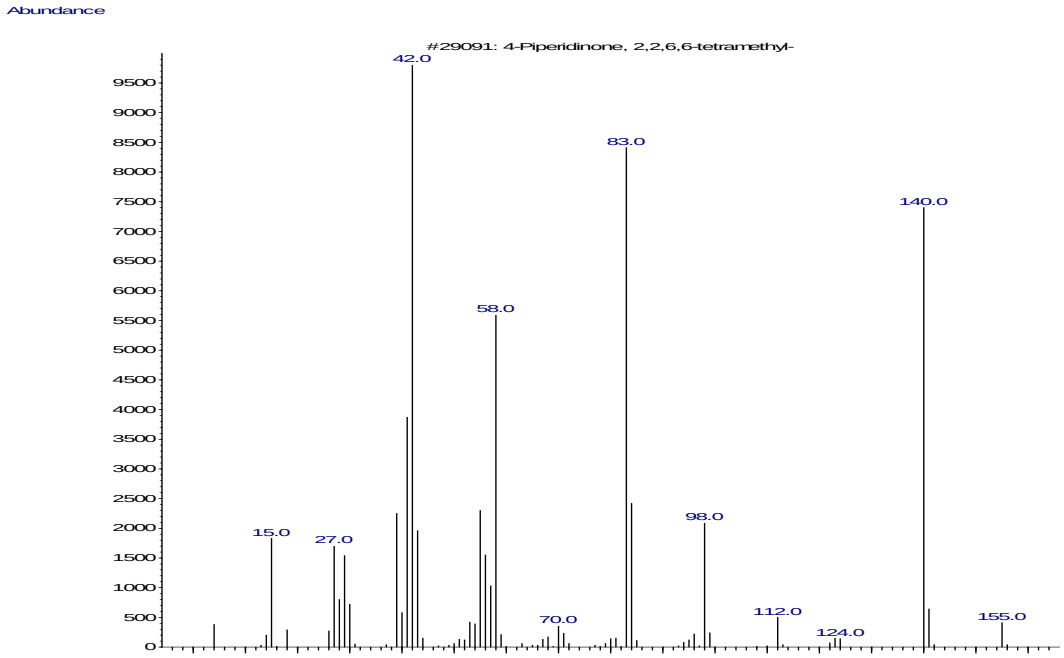

Fig. 3: 4-Piperdinone,2,2,6,6-tetramethyl. Chromatogram of the major constituents of [BMIM][Cl]

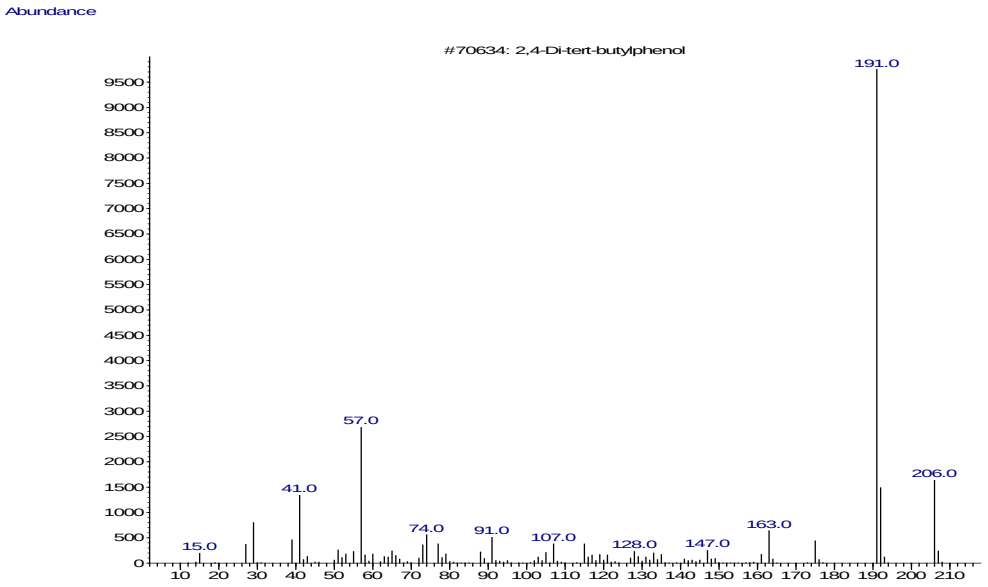

Fig. 4: 2,4-Di-tert-butylphenol. Chromatogram of the major constituents of [BMIM][Cl]

3.3 Surface Study of Aluminium Alloy in KOH

Scanning electron microscope is a type of microscope that produces images of a sample by scanning the surface with a focused beam of electrons (Anadebe et al, 2019). The electrons interact with atoms in the sample, producing various signals that contain information about the surface topography and composition of the sample. AA previously treated and polished was immersed in a beaker containing 1 M KOH solution in the absence and presence of [BMIM][Cl] inhibitor at 313 K for 3 hr. time duration The immersion of the aluminium alloy coupons into the IL inhibitor was done to ascertain the extent of damages done by the alkaline solution on the metals in the absence and presence of the inhibitors at that temperature and time. Scanning electron microscopy was carried out on both the non-inhibited and inhibited AA. Figure 5 (a) shows the micrograph of corroded surface of AA specimen in the absence of [BMIM][Cl] in 1 M KOH. Figure 5 (b) shows the micrograph of corroded surface of AA specimen in the presence of [BMIM][Cl] in 1 M KOH. The AA in uninhibited solution of KOH was strongly damaged due to the reaction between the free electrons on the metals and mobile electrons existing within the solution of immersion. But when the inhibitor was introduced into the solution the rate of reaction was retarded and eventually stops due to the formation of a thin film layer on top of the metal which separates the metal from the aggressive environment and thereby protects AA from further attack by the alkaline solution. In this process the life span of AA can be prolonged and prevented from sudden degradation. The inhibition is as a result of blocking the cathodic and anodic sites of the metal by the inhibitor molecules in the alkaline solution (Onukwuli and Omotioma, 2016; Ezeugo et al, 2017).

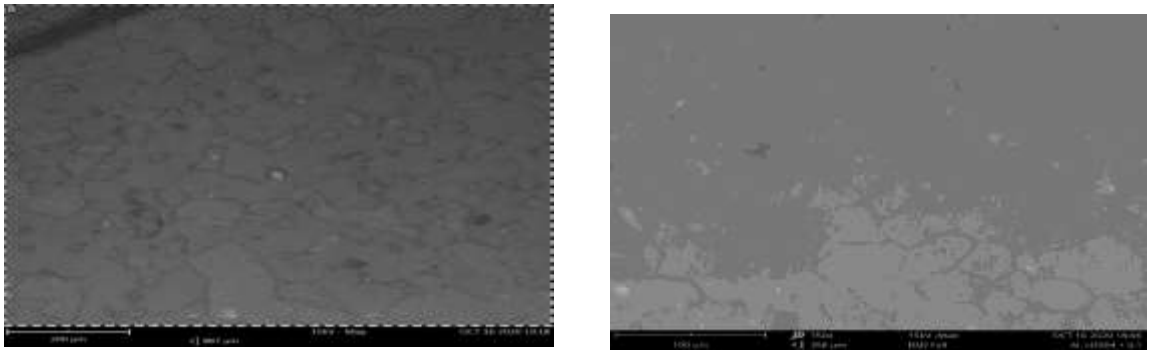

(a) (b)

Fig 5: The monographs of corroded AA specimen in 1 M KOH: (a) in the absence of [BMIM][Cl], (b) in the presence of [BMIM][Cl].

3.4 Results of Thermometric Method

The experiment was carried out using a thermostat set at initial temperature of 30 °C for the metal alloy and alkaline (KOH) medium. The reaction numbers were determined in the presence and in the absence of the IL concentrations. In each case, the value of the reaction number was determined as a function of the ratio of change in temperature to the maximum time reached (Udeh et al, 2021). The operational effects of the concentration of the IL on the reaction number and inhibition efficiency of the inhibitors was shown in Tables 1. The concentrations of the IL ranged from 0.2 to 1.0 g/L. The inhibition efficiency of the IL in alkaline medium was obtained as a function of reaction number in the absence (blank) and presence of the IL. Increase in the concentration of the IL, increases the inhibition efficiency of the inhibitor (Udeh et al, 2021). Increase in reaction number, decreases the value of the inhibition efficiency. This shows that inhibition efficiency is inversely related to the reaction number (RN). This is in agreement with investigation made by Omotioma and Onukwuli (2016) and Udeh et al, (2021). The maximum inhibition efficiency (IE %) obtained for the corrosion of AA in 1 M KOH solution at 303 K was 86.76 % at inhibitor concentration of 1.0 g/L and reaction number of 0.0512. Based on Figure 6 a slope value of -258.7597, correlation coefficient (R^2) value of 1 (unity) and intercept of 100.0109 was obtained which signifies strong relationship.

Table 1: Effect of [BMIM][Cl] on the IE (%) of AA in 1 M KOH solution at 303 K

Inhibitor conc. (g/L)	RN	IE (%)
0.0	0.3866	-
0.2	0.2033	47.40
0.4	0.1516	60.79
0.6	0.0928	76.00
0.8	0.0667	82.75
1.0	0.0512	86.76

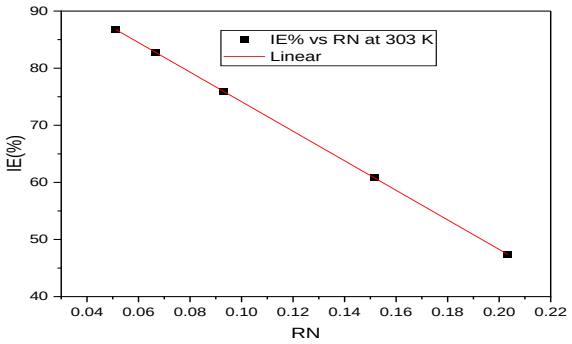

Fig. 6: Plot of IE (%) vs RN for the corrosion of AA in 1 M KOH at different concentration of [BMIM][Cl] at 303 K.

3.4.1 Potentiodynamic Polarization Method

The technique helps to determine the type of inhibitor with regards to cathodic and anodic polarization. The effect of [BMIM][Cl] on aluminium alloy dissolution reaction and hydrogen evolution reaction. The polarization curve for the investigated of AA in 1 M KOH solution is shown in Figure 7. The rapid dissolution of the metal alloy was observed in the absence of the inhibitor. The cathodic and anodic reaction was affected after addition of the inhibitor to the alkaline medium, but the cathodic reaction was more polarized for the metal in the presence of the IL as illustrated in Figure 7. A reverse shift on the cathodic and anodic curves was observed implying a decrease in the corrosion current density values, compared to the uninhibited solution. The depletion of the cathodic and anodic current implies that the inhibitor was mixed type (Talha et al, 2020). This observation envisaged that the inhibitor introduced in the aggressive solution retarded the anodic dissolution of the metals and cathodic hydrogen evolution (Deepa and Padmalatha, 2014). This trend increase with increasing the concentration of the inhibitor and also, higher concentration of the inhibitor leads to an elevated inhibition efficiency which was attributed to higher surface coverage of the inhibitor molecules on the metal surface.

Furthermore, the inhibitor may be classified as cathodic or anodic type if the displacement in E_{corr} value on addition of the inhibitor is greater than 85mV with respect to the corrosion potential of the blank (Zheng et al, 2015; Maduabuchi et al, 2017). When the displacement is less than 85 mV, the inhibitor may be considered to be mixed-type (Verma et al, 2018: Wang et al, 2020). Experimental results confirmed [BMIM][Cl] inhibitor as mixed-type inhibitor with predominantly cathodic effectiveness due to the corrosion potential value of - 452.6 mV/SCE. The maximum inhibition efficiency (Eq.3) obtained was 82.1% at inhibitor concentration of 1.0 g/L, temperature of 303 K, corrosion current density of 37.7 ($\mu A/cm^2$) and surface coverage of 0.821. The high inhibition efficiency of this IL may be attributed to the ease of adsorption of the inhibitor molecules on the surface of the aluminium alloy, the high molecular planarity of the heterocyclic compounds of the IL, the presence of electron donation groups and aromatic rings (Verma et al, 2019). The corrosion potential value (E_{corr}) and corrosion current density value (I_{corr}) estimated from the polarization curve and the calculated inhibition efficiency for different concentrations of the inhibitor are summarized in Table 2.

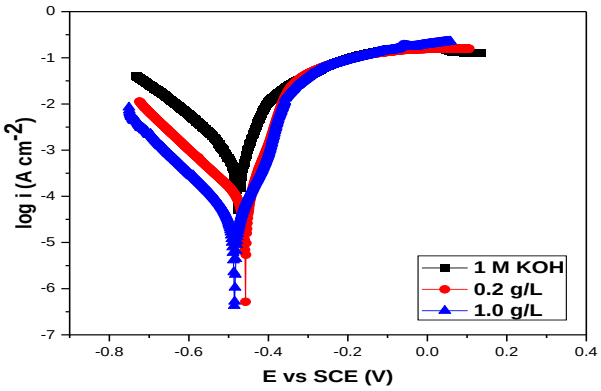

Fig. 7: Potentiodynamic polarization plots of AA in 1 M KOH environment in the absence and presence of [BMIM][Cl].

Table 2: Polarization parameters for AA in 1 M KOH at 303 K in the absence and presence of [BMIM][Cl]

System	E_{corr} (mV/SCE)	I_{corr} (µA/cm^2)	θ	IE (%)
KOH	-445.7	246.7	-	-
0.2 g/L IL_1	-440.5	67.6	0.726	72.6
1.0 g/L IL_1	-452.6	37.7	0.821	82.1

3.4.2 Electrochemical impedance Specroscopy (EIS) Method

The impedance spectra obtained for AA in 1 M KOH solution at 303 K with different concentrations of [BMIM][Cl] and 3 hrs.immersion are presented as Nyquist, bode phase angle and bode modulus plots in Figures 8a-8c. Figure 8d indicates the Circuit model for the EIS measurement of AA in 1 M KOH solution in the absence and presence of [BMIM][Cl]. The electrochemical impedance parameters derived from these studies are revealed in Table 3. The Nyquist plot revealed a semicircle with a punctuated identical projection nature all over the frequency studied signifying that the corrosion of aluminium is largely managed by charge transfer mechanism at electrode/electrolyte interface (Li et al, 2019; Verma et al, 2019). The flaw appearance of the capacitive loop may be attributed to the pitting and heterogeneous surface of the aluminium alloy in 1 M KOH (Namrata et al, 2017). It was observed that the capacitive loop increases with an increase in the concentration of [BMIM][Cl] in 1 M KOH solution. The loop intensifies with rise in the concentration of [BMIM][Cl] which validates the corrosion of AA is inhibited productively (El-Mahdy et al, 2015). However, reports have it that the inductive loop in the EIS spectra could be attributed to the adsorption and desorption equilibrium of surface-active moites or corrosion inhibitors on the AA surface (Hachelef et al, 2016). Other reports have it that the interrupting nature of the inductive loop may be attributed to the existence of the formation of passive film oxide at the surface of AA (Deepa and Padmalatha, 2014). An equivalent circuit shown in Figure 8d was introduced for the computation of the impedance parameters. The equivalent circuit comprised of solution resistance ($R_{(s)}$), charge transfer resistance ($R_{(t)}$) and the constant phase element (CPE) placed in parallel to the charge transfer resistance. The double layer capacitance (C_{dl}) was calculated at the maximum frequency (f_{max}) at which the imaginary part of the Nyquist plot is highest using Equation (5)

$$C_{dl} = \left[\frac{1}{2\pi f_{max} R_{(t)}}\right] \quad (5)$$

Where f_{max} is the maximum frequency of which the imaginary value reaches the maximum on the Nyquist plot. The value of the inhibition efficiency and surface coverage (θ) are calculated from the charge transfer resistance ($R_{(t)}$) using Eq. (4) (Jafari et al, 2014; Fouda and El-Haddaad, 2015; Namrata et al, 2017). The divergence of the bode modulus and phase angle at intermediate frequencies reveals the adsorption of [BMIM][Cl] molecules on the AA surface in 1 M KOH solution (Fouda et al, 2015). Also, the CPE is usually defined by two variables Q and n and the impedance of the CPE (Z) is denoted by Equation (6) (Li et al, 2019).

$$Z_{CPE} = \left[\frac{1}{Q(j\omega)^n}\right] \quad (6)$$

Where Q represents the proportionality constant due to the capacitance, j is the imaginary unit and ω is the angular frequency ($\omega = 2\pi f, f$ is the frequency at maximum in Hz) and n is the phase shift.

Table 3: Electrochemical parameters of AA in 1 M KOH without and with [BMIM][Cl] at different temperatures

C (g/L)	$R_{(t)o}$ (Ω cm^2)	$R_{(t)}$ (Ω cm^2)	IE (%)	f_{max} (Hz)	C_{dl}
At 313 K					
0.0	84.6	-	-	1213.0	1.551
0.2	-	246.3	65.60	1226.0	0.527
0.4	-	253.3	66.60	1528.0	0.399
0.6	-	260.9	67.60	1580.0	0.388
0.8	-	273.0	69.01	1592.6	0.366
1.0	-	289.8	70.80	2145.0	0.256
At 313 K					
0.0	80.2	-	-	1256.2	1.580
0.2	-	144.4	44.46	1197.6	0.920
0.4	-	215.6	62.80	1210.1	0.610
0.6	-	223.4	64.10	1224.1	0.582
0.8	-	246.7	67.49	1688.6	0.382
1.0	-	261.3	69.31	1985.7	0.287

3.5 Adsorption Mechanism

The adsorption activities of [BMIM][Cl] molecules on aluminium alloy surface can be investigated using different types of adsorption isotherms; Langmuir,Temkin, Frumkin and Florry-Huggins isotherms. However, to obtain the isotherms, the degree of surface coverage (θ) as a function of the inhibitor concentration was computed from the charge transfer resistance using Equation (7). (Hachelef et al, 2016)

$$\theta = \left[1 - \frac{R_{(to)}}{R_{(t)}}\right] \quad (7)$$

Where $R_{(to)}$ and $R_{(t)}$ are the charge transfer resistance in the absence and in the presence of the inhibitor, respectively. However efforts were made to test the various adsorption isotherms mentioned earlier with the values of the degree of surface coverage obtained from the adsorption of [BMIM][Cl] on AA surface. Langmuir adsorption isotherm was found to be the best fit and is represented by Equation (8). (Onukwuli and Omotioma, 2016; Udunwa et al, 2017).

$$\frac{C_{inh}}{\theta} = \frac{1}{K_d} + C_{inh} \quad (8)$$

Where C_{inh} is the concentration of the inhibitor in g/L, K_d is the adsorption or desorption equilibrium constant in L/g, the free energy of adsorption (ΔG_{ads}) was evaluated using Equation (9). (El-Mahdy et al, 2015; Anadebe et al, 2020; Ezeugo et al, 2018).

$$\Delta_{ads} = -RTIn(55.5K_d) \quad (9)$$

From the Langmuir parameters presented in Table 4, a graph of $\frac{C_{inh}}{\theta}$ against C_{inh} for the adsorption of [BMIM][Cl] on the surface of AA is ploted for different concentration of the inhibitor at 303 and 313 K. The graphs are presented in Figure 9, and indicates a linear graph with slopes ranging from 1.38685 to 1.26725, intercept 0.04085 to 0.16983 and correlation coefficients (R^2) values of 0.99905 and 0.99634 (close to unity) which validates the langmuir adsorption isotherm for the corrosion of AA in 1 M KOH solution at 303 and 313 K (Hachelef et al, 2016). The value of the adsorption constant (K_d) was evaluated from the intercept and was used to calculate the free energy of adsorption (Δ_{ads}) (Anadebe et al, 2020; Verma *et al*, 2019). The heat of adsorption operation of [BMIM][Cl] was calculated at 303 and 313 K using Equation. (10) (Nwabanne and Okafor, 2012; Udunwa et al, 2017; Anadebe et al, 2018). The heat of adsorption (Q_{ads}) was negative which suggests exothermic and spontanous interaction of the adsorbed molecules of [BMIM][Cl] on the aluminium alloy surface as shown in Table 5.

$$Q_{ads} = 2.303R\left[\log\left(\frac{\theta_2}{1-\theta_2}\right) - \log\left(\frac{\theta_1}{1-\theta_1}\right)\right] X\left(\frac{T_2 \times T_1}{T_2 - T_2}\right) \quad (10)$$

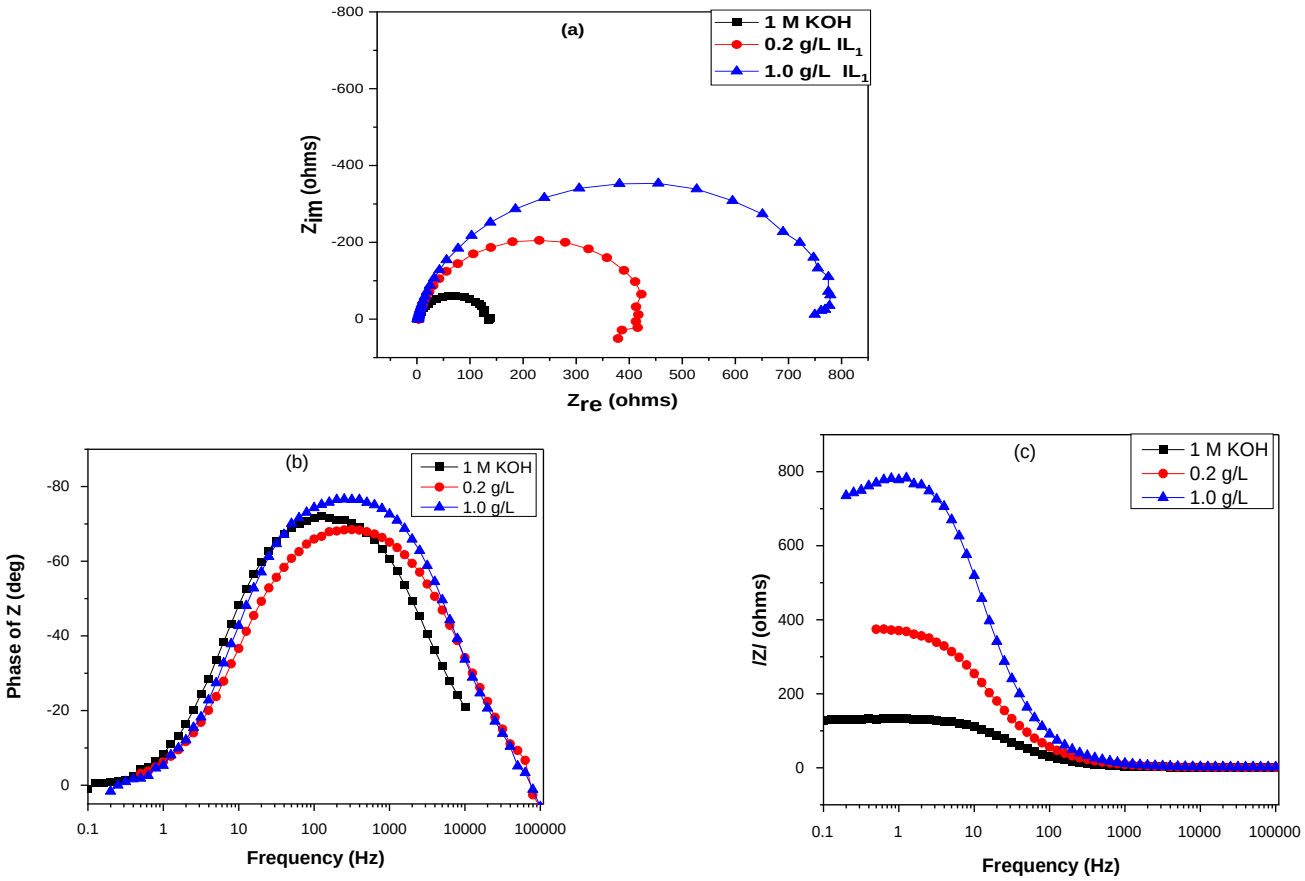

Fig. 8: Electrochemical spectra of AA in 1 M KOH environment in the absence and presence [BMIM][Cl] of (a) Nyquist (b) Bode phase (c) Bode mag.

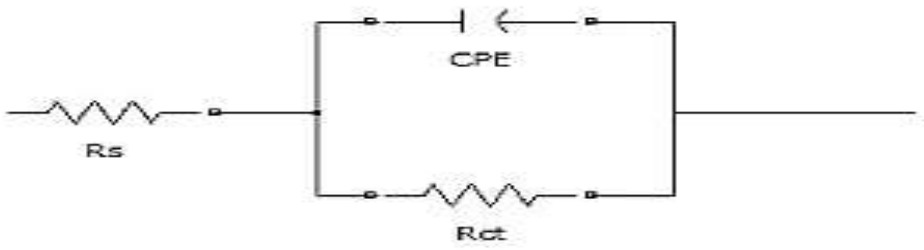

(d): Circuit model for the EIS measurement of AA in 1 M KOH solution in the absence and presence of [BMIM][Cl]

Table 4: Parameters of Langmuir adsorption isotherm at 303 K and 313 K for AA in 1 M KOH at different [BMIM][Cl] concentrations

C_{inh}(g/L)	C_{inh}/θ (g/L) 303 K	C_{inh}/θ (g/L) 313 K
0.0	-	-
0.2	0.3049	0.4498
0.4	0.6006	0.6369
0.6	0.8876	0.9360
0.8	1.1593	1.1854
1.0	1.4124	1.4428

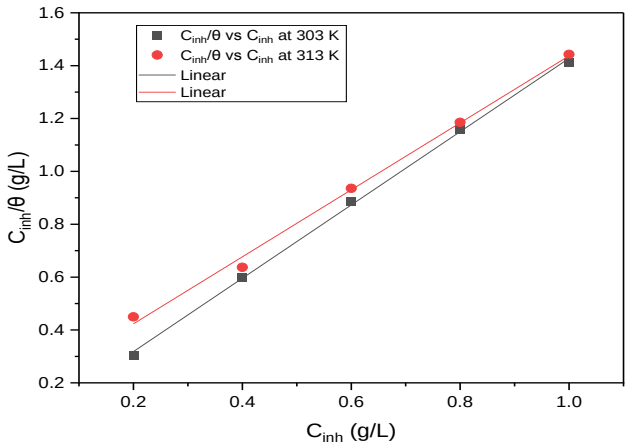

Fig. 9: Langmuir isotherm plot of C_{inh}/θ versus C_{inh} for AA in 1 M KOH containing different concentration of [BMIM][Cl]: at 303 K and 313 K

The negative value of Δ_{ads} devulged a spontaneous adsorption of [BMIM][Cl] molecules on the surface of the aluminium alloy and strong interaction of the moites in the electrolyte during the electrochemical process (Hachelef et al, 2016). Normally, the free energy threshhold for charge transfer or sharing from inhibitor molecules to the metal surface to form a co-ordinate type of bond is -40 kJ/mol. which is greater than the free energy of adsorption of the current study which is above -31.20 kJ/mol. manifesting physisorption mechanism. A process which permits electrostatic interaction among charged molecules and a charged metal (Hachelef et al, 2016).

Table 5: Adsorption parameters for the corrosion of AA in 1 M KOH solution at 303 and 313 K

Temperature K	K_d (L/g)	ΔG_{ads} (kJ/mol.)	Q_{ads} (kJ/mol.)	θ
303	24.480	-31.20	-1.688	0.7080
313	05.882	-28.50		0.6931

3.6 Temperature Effect

The effect of temperature on the corrosion inhibition of aluminium alloy in 1 M KOH was studied at 1.0 g/L [BMIM][Cl] concentration at 303 and 313 K. Table 6 revealed the result of the response of the charge transfer resistance with change in temperature. According the resultant data, charge transfer resistance decreases as the temperature rises. The reduction in the charge transfer resistance value leads to the decrease in the inhibition efficiency and increase in the double layer capacitance (El-Mahdy et al, 2015; Hachelef et al, 2016). It also decreases adsorption of the inhibitor and surface coverage.

Table 6: Electrochemical parameters for corrosion of AA in 1 M KOH containing 1.0g/L [BMIM][Cl].

Temperature K	$R_{(t)}$ (Ω cm^2)	f_{max} (Hz)	C_{dl}	IE (%)
303	289.8	2145.0	0.256	70.08
313	261.3	1985.7	0.287	69.31

4.0 Conclusions

An eco-friendly immidazolium based ionic liquid used as inhibitor for the corrosion of aluminium alloy in 1 M KOH was synthesized and characterized.

Electrochemical and thermometric techniques were employed for the investigation of the inhibitive performance of [BMIM][Cl] for aluminium alloy in 1 M KOH solution at different temperatures.

Results obtained from the potentiodynamic polarization revealed [BMIM][Cl] ionic liquid behaves as a mixed type inhibitor and protects aluminium alloy corrosion in 1 M KOH electrolyte solution.

The electrochemical impedance spectroscopy result demonstrated [BMIM][Cl] acts as a surface corrosion inhibitor for aluminium alloy and forms an unstable thick film on the metal's surface.

Increase in temperature of the electrolyte solution results to an increase in the values of the charge transfer resistance and double layer capacitance, while inhibition efficiency decreases.

Adsorption of [BMIM][Cl] on the surface of aluminium alloy obeys the langmuir adsorption isotherm and the value of the free energy of adsorption depicts physisorption operation

Nomenclature

Corrosion current density	I_{corr} ($\mu A/cm^2$)
Corrosion potential	E_{corr} (mV/SCE)
Charge transfer resistance	$R_{(t)}$ (Ω cm^2)
Free energy of adsorption	ΔG_{ads} (kJ/mol.)
Heat of adsorption	Q_{ads} (kJ/mol.)
Inhibitor concentration	C (g/L)
Inhibition efficiency	IE (%)
Maximum frequency	f_{max} (Hz)
Reaction number	RN (^oC/min.)

Refrences

Abiola, O. K., Oforka, N. C., Ebenso, E.E. 2007. Eco - friendly corrosion inhibitors: Inhibitive action of *Delonix regia* extract for the corrosion of aluminium in acidic medium. *Anti - Corrosion Methods and Materials*, 54, 219 - 224.

Anadebe, V. C., Onukwuli, O. D., Omotioma, M., Okafor, N. A. 2019. Experimental, theoretical modelling and optimization of inhibition efficiency of pigeon pea leaf extract as anti-corrosion agent of mild steel in acid environment. *Materials Chemistry and Physics,* 233, 120-132.

Anadebe, V. C., Onukwuli, O. D., Abeng, F. E., Okafor, N. A., Ezeugo, J. O., Okoye, C. C. 2020. Electrochemical kinetics, MD-simulation and multi-input single-output (MISO) modeling using adaptive neuro-fuzzy inference system (ANFIS) prediction for dexamethasone drug as eco-friendly corrosion inhibitor for mild steel in 2 M HCl electrolyte. *Journal of the Taiwan Institute of Chemical Engineers,* 115, 251-265.

Amitha Rani, B. E., Bharathi Baij, B, 2011. Green inhibitors for corrosion protection ofmetals and alloys. *International Journals of Corrosion,* 2012, 1 - 16.

Asadi, N., Ramezanzadeh, M., Bahlakeh, G., Ramezanzadeh, B. 2019. Utilizing lemon balm extract as efficient green corrosion inhibitor for mild steel in 1 M HCl solution: a detailed experimental, molecular dynamics, Monte Carlo and quantum mechanics study. *Journal of the Taiwan Institute of Chemical Engineers,* 100, 239-251.

Chauhan, D.S., Verma, C., Quraishi, M.A. 2021. Molecular structural aspects of organic corrosion inhibitors: Experimental and computational insight. *Journal of Molecular Liquids,* 1227, 129374.

Devarayan, K., Mayakrishnan, G., Nagarajan, S. 2012. Green inhibitors for corrosion of metals. *Chemical, Science Review and lett*ers, 1 (1) 1 - 8.

Dharaskar, S.A., Wasewar, K.L., Varma, M.N., Shende, D.Z., Yoo, C. 2013. Synthesis, characterization and application of 1-buthyl-3-methylimidazolium tetraflouroborate for extraction desulphurization of liquid fuel. *Procedia Engineering,* 51, 416-422.

Deepa, P., Padmalatha, R. (2014). Corrosion behaviour of 6063 aluminium alloy in acidic and in alkaline media. *Arabian Journal of Chemistry*, 1-13.

Dehghani, A., Bahlakeh, G., Ramezanzadeh, B. 2019. Green eucalyptus leaf extract: A potent source of bio-active corrosion inhibitors for mild steel. *Bioelectrochemistry*, 130. 107339- 107342

El-Mahdy, G.A., Atta, A.M., Al-Lohedon, H.A., Ezzar, A.O. 2015. Influence of green corrosion inhibitor based chitoson ionic liquid in the steel corrobility in chloride solution. *International Journal of Electrochemical Science,* 10, 5812-5826.

Ejikeme, P. M., Umana, S. G., Menkiti, M. C., Onukwuli, O. D. 2015. Inhibition of mild steel and aluminium corrosion in 1M H_2SO_4 by leaves extract of African breadfruit. *International Journal of Materials and Chemistry,* 5 (1), 14-23.

Emembolu, L. N., Onukwuli, O. D., Okafor, V. N. 2020. Characterization and optimization study of *Epiphyllum oxypetallum* extract as corrosion inhibitor for mild steel in 3 M H_2SO_4 solutions. *World Scientific News,* 145, 256-273.

Ezeugo, J. N. O., Onukwuli, O. D., Omotioma, M. 2017. Optimization of corrosion inhibition of *Picralima nitida* leaves extract as green corrosion inhibitor of zinc in 1.0 M HCl. *World News of Natural Sciences,* 15, 139-161.

Eddy, N.O., Ameh, P., Gimba, C.E., Ebenso, E. 2011. GCMS studies on *Anogessus leocarpus* (Al) gum and their corrosion inhibition potential for mild steel in 0.1 M HCl. *International Journal of Electrochemical Science,* 6 (11), 5815-5829.

Ezeugo, J. N. O., Onukwuli, O. D., Omotioma, M. 2018. Inhibition of aluminium corrosion in 1.0 M HCl using *Picralima nitida* leaves extract. *Der Pharma Chemica,* 10 (SI), 7-13.

Fouda, A.S., El-Haddad, M.N. 2015. The potential of 1,2,3-benzotriazole in inhibiting corrosion of aluninium in acid media. *International Journal of Chemistry and Material Science,* 3 (2), 033-042.

Hachelef, H., Benmousat, A., Khelifa, A., Athmani, D., Bonchereb, D. 2016. Study of corrosion inhibition by electrochemical impedance spectroscopy method of 5083 aluminium alloy in 1 M HCl solution containing propolis extract. *Journal of Material and Environmental Science,* 7 (5), 1751-1758.

Jafari, H., Danaee, I., Eskandari, H., Rashvandavei M. 2014. Combined computational and experimental study on the adsorption and inhibition effects of N_2O_2 schiff base on the corrosion of API 5L grade B steel in 1 mol/L HCl. *Journal of Material Science Technology,* 30, 239-52.

Li, X., Deng, S., Fu, H. 2011. Inhibition by tetradecylpyridinium bromide of the corrosion of aluminium in hydrochloric acid solution. *Corrosion Science,* 53, 1529-1536

Li, Y., Zhang, S., Ding, Q., Qin, B., Hu, L. 2019. Versatile 4,6-dimethyl-2- mercaptopyrimidine based ionic liquid as high- performance corrosion inhibitors and lubricants. Journal of Molecular Liquids, 284, 577-585.

Maduabuchi, A.C., Oguzie, E.E., Liu, L., Li, Y. 2017. Inhibitory action of Funtumia elastic extracts on the corrosion of Q235 mild steel in hydrochloric acid medium: Experimental and theoretical studies. *Journal of Dispersion Science and Technology,* 36 (8), 1126-1136.

Namrata, C., Savita, S., Singh, V.K., Quraishi, M.A. 2017. Corrosion inhibition performance of different bark extracts on aluminium in alkaline solution. *Journal of the Association of Arab Universities for Basic and Applied Sciences,* 22, 38- 44.

Ndibe, O. M., Menkiti, M. C., Ijomah, M. N. C., Onukwuli, O. D. 2011. Corrosion inhibition of mild steel by acid extract of *Vernonia amygdalina* in HCl and HNO_3. *Electronic Journal of Environmental, Agricultural and Food Chemistry,* 10 (9), 2847-2860.

Njoku, C.N., Onyelucheya, O.E. 2015. Response surface optimization of the inhibition efficiency of *Gongronema latifolium* as an inhibitor for aluminium corrosion in HCl solution. *International Journal of Materials and Chemistry,* 5 (1), 4-13

Nnanna, A.L, Nwadiuko, C.O., Ekekwe, D.N., Ukpabi, F.C., Udensi, C.S., Okeoma, B.K., Onwuagba, N.B., Mejeha, M.I. 2011. Adsorption and inhibitive properties of leaf extract of *Newbouldia leavis* as a green inhibitor for aluminium alloy in H_2SO_4. *American Journal of Materials Science,* 1 (2), 143-148.

Nwabanne, J.T., Okafor, V.N. 2012. Adsorption and thermodynamic study of the inhibition of corrosion of mild steel in H_2SO_4 medium using *Veronia amygdalina. Journal of Minerals and Materials Characteristics and Engineering,* 11, 885-890.

Okafor, C. S., Anadebe, C. V., Onukwuli, O. D. 2019. Experimental, statistical modelling and molecular dynamics simulation concept of *Sapium ellipticum* leaf extract as corrosion inhibitor for carbon steel in acid environment. *South African Journal of Chemistry,* 72, 164-175.

Omotioma, M., Onukwuli, O. D. 2016. Modelling the corrosion inhibition of mild steel in HCl medium with the inhibition of pawpaw leaves extract. *Portugaliae Electrchimica Acta,* 34 (4), 287-294.

Onukwuli, O. D., Omotioma, M. 2016. Optimization of the inhibition efficiency of mango extract as corrosion inhibitor of mild steel in 0.1 M H_2SO_4 using response surface methodology. *Journal of Chemical Technology and Metallurgy,* 51 (3), 302-314.

Onukwuli, O. D., Omotioma, M. 2019. Study of bitter leaves extract as inhibitive agent in HCl medium for the treatment of mild steel through prickling. *Portugaliae Electrochimica Acta,* 37 (2), 115-121.

Onukwuli, O. D., Ezeugo, J. O. 2018. Plant extract as biodegradable inhibitor for zinc in dilute solution of sulphuric acid. *World Scientific News,* 109, 195-210.

Sasikumar, Y., Adekunle, A.S., Olasunkanmi, L.O., Bahadur, I., Baskar, R., Kabanda, M.M., Obot, I.B., Ebenso, E.E. 2015. Experimental, quantum and Monte-Carlos simulation studies on corrosion inhibition of some alkyl immidazolium ionic liquids containing tetraflouroborate anion on mild steel in acid medium. *Journal of Molecular Liquids,* 211, 105-118.

Shetty, S.K., Shetty, A.N. 2015. Ionic liquids as an effective corrosion inhibitor on 6061 Al-15 vol. pct. sic (p) composite in 0.1 M H_2SO_4 medium-an eco-friendly approach. *Canadian Chemical Transactions,* 3, 41-64.

Singh, A., Quraishi, M.A. 2012. Aswain (Trachyspermum copticum) seed extract as efficient corrosion inhibitor for aluminium in NaOH solution. *Research Journal of Recent Sciences,* 2011, 57-61.

Talha, M., Wang, X., Liu, H., Huang, A., Lin, D., Lin, Y. 2020. Imidazolium-based ionic liquid as an efficient corrosion inhibitor for AA 6061 alloy in HCl solution. *Materials,* 13, 4672- 4679.

Terrence, B. (2016). Metthods of corrosion prevention on metals. ASM Handbook, 13, 668 -679.

Udeh, B.C., Onukwuli, O.D., Omotioma, M. 2021. Application of metronidazole drug as a corrosion inhibitor of mild steel in hydrochloric acid medium. *Journal of Engineering and Applied Science,* 10 (1), 2327-347.

Udunwa, D. I., Onukwuli, O. D., Omotioma, M. 2017. Corrosion control of aluminium alloy in HCl using extract of Ocimum gratissimum as inhibitor. *Der Pharma Chemica,* 9 (19), 48-59.

Verma, C., Ebenso, E.E., Quraishi, M.A. 2017. Ionic liquids as green and sustainable corrosion inhibitors for metals and alloys: An overview. *Journal of Molecular Liquids,* 233, 403-414.

Verma, C., Quraishi, M.A., Ebenso, E.E., Indra, B. 2018. A green and sustainable approach for mild steel acidic corrosion inhibition using leaves extract: experimental and DFT studies. *Journal of Bio and Tribo - Corrosion,* 4 (3), 1-12.

Verma, C., Olasunkanmi, L.O., Bahadur, I., Lgaz, H., Quraishi, M.A., Haqure, J., Sherif, M., Ebenso, E.E. 2019. Experimental, density functional theory and molecular dynamics supported adsorption behaviour of environmental benign imidazolium based ionic liquids on mild steel surface in acidic medium. *Journal of Molecular Liquids,* 27, 1-5.

Wang, X., Huang, A., Lin, D., Talha, M., Liu, H., Lin, Y.(2020. Imidazolium-based ionic liquid as efficient corrosion inhibitor for AA 6061 alloy in HCl solution. *Materials,* 13, 4672- 4690.

Zhang, Q., Hua, Y. 2010. Corrosion inhibition of aluminium in hydrochloric acid solution by alkylimidazolium ionic liquids. *Material Chemistry and Physics,* 119 (1), 57-64

Zheng, X., Zhang, S., Li, W., Gong, M., Yin, L. 2015. Experimental and theoretical studies of two imidazolium-based ionic liquids as inhibitors for mild steel in sulphuric acid solution. *Corrosion Science,* 95, 168-179.